HHS Public Access

Author manuscript

*Adv Oncol*. Author manuscript; available in PMC 2023 April 14.

Published in final edited form as:

*Adv Oncol*. 2021 May ; 1: 29–39. doi:10.1016/j.yao.2021.02.003.

# MRI-Guided Radiation Therapy

**Sangjune Laurence Lee, MD, MSE, FRCPC**[a,b], **William A. Hall, MD**[c], **Zachary S. Morris, MD, PhD**[a], **Leslie Christensen, MA**[d], **Michael Bassetti, MD, PhD**[a,*]

[a]Department of Human Oncology, University of Wisconsin Hospital and Clinics, Madison, WI, USA;

[b]Department of Oncology, Division of Radiation Oncology, University of Calgary, Calgary, AB, Canada;

[c]Department of Radiation Oncology, Medical College of Wisconsin, Milwaukee, WI, USA;

[d]University of Wisconsin School of Medicine and Public Health, Madison, WI, USA

**Keywords**

MR-guided radiation therapy; MR guidance; MR linear accelerator; MR-linac; MRIgRT; Plan adaptation; Real-time imaging

## INTRODUCTION

The development of the integrated MRI-guided radiotherapy systems (MRIgRT) is an engineering feat with growing adoption in hospitals over the past 6 years. Currently, there are 2 MRIgRT systems in development, and 2 systems that are commercially available [1–4]. ViewRay (Cleveland, OH) was the first to market with a 0.35-T MRI combined with a radioactive cobalt system in 2014 that has since been upgraded to linear accelerator–based photon radiation (MR-linac) [2,5]. Elekta treated its first patient with the 1.5-T MR-linac system in 2017 [6].

Unlike the cone beam computed tomography (CBCT)-based linear accelerator, MRIgRT can provide continuous real-time, high soft tissue contrast imaging while radiation is being delivered. This enables daily adaptation of the radiation plan according to changes in daily anatomy, and real-time respiratory gating. In many circumstances, MRIgRT may therefore allow for tighter treatment margins and this has the potential to enable safe delivery of higher doses per fraction. This could translate into better tumor control, less radiation toxicity, and/or fewer treatment visits.

The purpose of this review was to survey the inroads that the MRIgRT has made in the treatment of cancers in certain anatomic locations and to discuss new opportunities for

*Corresponding author. Department of Human Oncology, University of Wisconsin, University Hospital L7/B36, 600 Highland Avenue, Madison, WI 53792. Bassetti@humonc.wisc.edu.

SUPPLEMENTARY DATA

Supplementary data related to this article can be found online at https://doi.org/10.1016/j.yao.2021.02.003.

Video content accompanies this article at http://www.advances-oncology.com/.

using MRIgRT to provide more effective radiation therapy. For each body site, we highlight physics problems and technical challenges that should be considered when treating patients with MRIgRT.

## PANCREATIC CANCER AND ONLINE ADAPTIVE RADIOTHERAPY

Improvements in the effectiveness of systemic therapy increase the importance of local therapy for pancreatic cancer through dose-escalation strategies of intact tumors [7]. Because of the close proximity and interfraction motion of the duodenum and stomach to the pancreas, stereotactic ablative radiotherapy (SABR) for pancreatic cancer is difficult, with the rate of grade 2 or higher gastrointestinal (GI) acute toxicity between 2% and 80% and late toxicity between 10% and 50% on convectional CBCT-based linear accelerators [8]. The main advantage of treating patients with pancreatic cancer with MRIgRT may be its ability to perform online plan adaptation [9]. In CBCT-based treatments, a single radiotherapy plan is designed and used for all fractions because of the inability to visualize the changing anatomy of the pancreas and surrounding luminal organs. With the MR-linac, the radiation plan can be adapted while the patient is on the treatment table before the delivery of each fraction so as to take into account the changing anatomy of the day [10]. Plan adaptation is more time-consuming and labor-intensive than the CBCT-based workflow, but can be expedited by only recontouring organs at risk (OARs) within a 3-cm radius from the planning target volume (PTV) [11]. In studies in which all fractions are adapted, the chance that dose objectives are met increases from 43.9% to 83.0% [12].

In a study of 44 patients with unresectable pancreatic cancer treated with cobalt-based MRIgRT SABR, patients treated with a biological equivalent dose (BED) greater than 70 Gy had a 2-year overall survival of 49% versus 30% in those treated with a BED less than 70 Gy, with no grade ≥3 toxicities in the high-dose group [13]. A prospective, multi-institutional trial prescribing 50 Gy in 5 fractions with adaptive MRIgRT to patients with inoperable pancreatic cancer is currently under way (NCT03621644).

## OLIGOMETASTASES AND ISOTOXIC PLANNING

Improved imaging techniques, such as prostate-specific membrane antigen (PSMA) PET, and new laboratory testing, such as circulating tumor DNA, can improve the detection of metastatic disease, increasing the chance of improving overall survival when combined with the early use of SABR [14–16]. Several groups have reported their experiences with MRIgRT SABR for oligometastatic disease. In the study by Winkel and colleagues [17], 14 patients with oligometastatic disease in the pelvic or para-aortic region were treated with 35 Gy in 5 fractions. In the study by Palacios and colleagues [18], 84 patients with adrenal metastases were treated with breath-hold gating and a range of ablative doses depending on proximity to OARs. In the study by Henke and colleagues [19], 20 patients with abdominal metastases were treated with breath-hold gating and 50 Gy in 5 fractions. In all 3 studies, on-table adaptation significantly decreased OAR dose constraint violations and improved target coverage compared to without adaptation. Henke and colleagues [19] reported no grade ≥3 toxicities at 6 months of follow-up.

MRIgRT may improve the safety and efficacy of SABR by enabling isotoxic dose escalation. In conventional radiotherapy, planning objectives aim to cover the target with a homogeneous dose. In isotoxic dose escalation, the dose to the target is increased until the dose constraint of a proximal OAR is met, and the dose distribution over the target is highly heterogeneous. Heterogeneous dose coverage of the PTV minimizes the dose to OARs but requires better motion management compared with homogeneous dose coverage (Fig. 1) [20]. Isotoxic target dose escalation may improve survival outcomes, although clinical outcomes from thoracic treatments have been mixed [21–23].

## CENTRAL NERVOUS SYSTEM CANCERS AND IMAGING BIOMARKERS

MRI is already incorporated in the workflow for the treatment of central nervous system (CNS) malignancies and metastases due to its ability to visualize and distinguish normal brain and intracranial tumors. MRIs are rigidly registered to the planning CT scan to guide highly conformal stereotactic radiosurgery (SRS), SABR, and fractionated stereotactic radiotherapy (FSRT) radiation plans, often in 1 to 5 fractions in the case of brain metastases and spine metastases [24]. SABR to spinal bone metastases can provide improved local control compared with conventional radiation [25]. To avoid damaging the spinal cord, patients typically require a diagnostic-quality MRI to be rigidly fused to a CT. Both images must be acquired while the patient is fixed into position in a rigid mold. A pilot trial at Washington University in St. Louis is exploring the feasibility of delivering spine SABR on the same day as simulation on the MR-linac, reducing the duration between simulation and treatment, which can be several days (NCT03878485). Although promising, obtaining the highly conformal radiation dose distributions needed for SABR on MRIgRT units can be difficult because non-coplanar beams/arcs are not possible with currently available devices.

Treating CNS malignancies with the MRIgRT opens opportunities to understand changes in the tumor biology during treatment with advanced MRI pulse sequences due to relative lack of motion at this body site. The treatment of 3 patients with glioblastoma with cobalt-based MRIgRT was demonstrated by Mehta and colleagues [26] and showed changes in the postoperative cavity and cerebral edema volumes during the 6-week course of radiation therapy. By manipulating the MRI acquisition parameters, information regarding tumor cellularity, vascularity, and biochemical makeup can be gathered [27]. Although advanced pulse sequences have higher signal-to-noise ratio at 1.5 T, research is under way to incorporate these pulse sequences into 0.35-T MR-linacs [28]. In the treatment of glioblastoma, advanced imaging can identify areas at higher risk of recurrence for radiation-boosting strategies [29]. MRI imaging biomarkers could also introduce a paradigm shift in the target dose objectives. Traditionally, a single homogeneous dose was recommended for treating the tumor. Advanced physiologic imaging could identify higher-risk areas within the tumor and provide rationale for heterogeneous dose distribution [30]. Instead of treating each tumor to a fixed dose, treatment could be given until an MRI biomarker that is strongly correlated with outcomes reaches a certain threshold (Fig. 2) [31]. Use of injectable agents, such as prostate-specific membrane antigen-targeted nanoplexes that are both therapeutic and diagnostic under MRI, is an emerging field that could help focus radiation treatment to high-risk areas [32].

## HEAD AND NECK CANCER AND DEEP LEARNING ENABLED AUTO-CONTOURING

Although radiation therapy plays an integral role in treating head and neck (HN) malignancies, delivery of radiation is difficult because of the close proximity to radiation-sensitive normal tissues. In a study by Raghavan and colleagues [33] of 6 patients treated with cobalt-based MRIgRT, the primary tumor and parotid gland volumes decreased, and their positions shifted significantly during the 7 weeks of radiation therapy. Chen and colleagues [34] reported on 18 patients with HN primaries treated with cobalt-based MRIgRT with disease control and quality-of-life outcomes similar to conventional CBCT-based radiation therapy. However, even with improved visualization of the tumor and OARs with daily MRI, only a minority of patients required plan adaptation [34]. Because the anatomy of the HN can change over weeks during radiation treatment, several investigators are exploring the use of weekly MRIs for plan adaptation to more accurately target the tumor and spare OARs (NCT03972072) [35].

In the traditional workflow, a patient undergoes a simulation scan, which is used to contour the target and OARs. The distribution of beams and physics quality checks are based on these contours. This process usually takes several days. For HN plans, the contouring can be especially time-consuming due to complex anatomy. Deep learning may help decrease the amount of work required for contouring. Deep learning is a field of artificial intelligence in which computers learn how to produce contours based on a previously created set of contoured images [36,37]. Deep learning has been applied to CTs of the HN to automatically contour the tumor and high-risk expansion volumes as well as OARs [38,39]. In a study by Tong and colleagues [40], twenty-five 0.35-T MRIs were used to develop a deep learning algorithm to contour bony and soft tissue OARs in the HN.

## BREAST CANCER AND THE ELECTRON RETURN EFFECT

Hypofractionated radiation is the standard of care for early-stage breast cancer with whole breast adjuvant therapy and is gaining acceptance with locoregional therapy for more advanced disease [41–43]. Accelerated partial breast irradiation (APBI) can limit the radiation field to the postoperative bed with acceptable local control and cosmesis compared with hypofractionated whole breast treatments [44,45]. As targeting becomes more focused and fractionation schedules become shorter, MRI studies suggest that tracking the position of the breast and the volume of the seroma become more critical [46,47]. Investigations are being conducted to determine whether neoadjuvant MRIgRT could reduce the volume of normal breast tissue irradiated or detect a pathologic complete response [48,49]. Cobalt-based MRIgRT APBI has been used to treat patients with breast cancer, although long-term outcomes have not yet been reported [50,51]. Kennedy and colleagues [52] reported the use of single-fraction, adjuvant partial breast irradiation for 50 patients with early-stage disease, with most patients treated using cobalt-based MRIgRT. At 25 months' median follow-up, there were no grade ≥3 toxicities and no in-field recurrences [52]. The results of a prospective trial investigating the use of neoadjuvant single-fraction ablative radiation with an MRI simulation are currently pending [53].

One of the challenges facing MRIgRT in breast cancer is the electron return effect (ERE). When x-ray photons hit tissue within the body, a cascade of electrons is produced that generally travels in the same direction as the incident photons and eventually deposits free radicals that damage DNA. In the magnetic field of MRIgRT systems, the Lorentz force pushes the moving electron particles in a perpendicular direction with a force that is proportional to the magnitude of the magnetic field. Electrons that are given off from the tissue to the air circle back to the skin in what has been called the ERE (Fig. 3). Mitigating the ERE, which increases skin dose, is a challenge for MRIgRT, and is especially relevant for breast cancer treatment because of the importance of cosmesis. To avoid unwanted ERE irradiation outside the breast treatment fields, use of a 1-cm bolus shielding the upper torso is recommended for 0.35-T and 1.5-T MR-linacs [51,54]. The ERE has a larger impact on targets near an air-tissue interface, such as breast, lung, or GI cancers but can be minimized by taking the magnetic field effects into account during plan design [55,56].

## LUNG CANCER AND RESPIRATORY MOTION MANAGEMENT

SABR provides a high rate of local control, usually with minimal morbidity, for patients with medically inoperable early-stage lung cancer or metastases to the lung [57]. Although lung lesions are easy to see on CBCT, organs in the central mediastinum are better visualized on MRI. In a study of 5 ultra-central lung lesions, Henke and colleagues [58] reported no grade ≥3 acute toxicity within 6 months after cobalt-based MRIgRT. Finazzi and colleagues [59] reported the treatment of 54 patients with higher-risk lung lesions due to central location, re-irradiation, or interstitial lung disease with either cobalt-based or linac-based MRIgRT. At 12 months, local control was 95.6% with 8% grade 3 toxicities and no grade 4 to 5 toxicities.

MR-linacs may be able to achieve lower rates of toxicity with respiratory gating. In CBCT-based radiation, a volume containing all possible positions of the lung tumor during a respiratory cycle is typically irradiated. Although respiratory gating with a CBCT-based linear accelerator with techniques such as active breathing control is feasible, gating may be easier and more accurate on MRIgRT units because MRIgRT can image the tumor constantly throughout radiation treatment. Therefore, the treatment volume can be minimized by irradiating the tumor only when it is in a specific location during the respiratory cycle [60]. On the ViewRay system, a single sagittal slice constantly images the tumor. The patient is normally asked to perform a maximum inspiration breath-hold. The system is able to track the tumor as the patient breathes. The beams are turned on automatically when the tumor is within a certain window and turned off when the patient resumes respiration (Video 1). This process increases the delivery time of a single fraction but enables tighter treatment margins by eliminating the need for an internal target volume to account for tumor motion during respiration (Fig. 4).

## PROSTATE CANCER AND SYNTHETIC COMPUTED TOMOGRAPHY

Because prostate cancer has a low $\alpha/\beta$ ratio, hypofractionated treatments may improve the therapeutic ratio [61]. MR-guided radiation can allow for online adaptive replanning and can also inform dose escalation to intraprostatic lesions while avoiding the urethra. In a

study of 25 patients with mainly intermediate-risk prostate cancer treated with 35 Gy in 5 fractions with daily adaptation on a 1.5-T MR-linac, 16% of patients developed acute grade 2 GI or genito-urinary (GU) toxicity, and there were no grade ≥3 toxicities [62]. In another study of 101 patients with an even mix of intermediate-risk and high-risk prostate cancer treated with 36.25 Gy in 5 fractions with daily adaptation on a 0.35-T cobalt-based MRIgRT, the cumulative rate of acute grade 2 GI or GU toxicity was 28.8% without any grade ≥3 toxicities [63]

One way to shorten the overall radiotherapy workflow is to omit the CT scan. In the current workflow, the CT scan is registered to the MRI to provide electron density information, which is necessary for calculating dosimetry. However, errors in registration and changing anatomy can reduce accuracy. Alternatively, the MRI can be used to create a "synthetic CT." There are 2 broad categories of methods to create synthetic CTs. In voxel-based methods, information about the MRI voxel intensity, usually from 2 or more pulse sequences, is used to assign electron densities. These methods are less reliant on information about the location of the voxel within the MRI. Voxel-based methods are predominantly deep learning algorithms, in which the computer is given matched MRIs and CTs and then is able to create a CT from a new MRI. In atlas-based methods, the position of each MRI voxel is aligned to a predefined reference atlas of anatomic structures or set of reference atlases through image registration. Each structure in the atlas is assigned to a particular electron density value. Currently, there are 2 synthetic CT algorithms for prostate radiotherapy approved by the Food and Drug Administration [64]. The use of synthetic CTs could lead to more efficient workflows, in which the time between simulation and treatment is decreased from several days to a single day.

## GYNECOLOGIC MALIGNANCIES AND FIELD SIZE

The use of MRI for 3-dimensional high-dose-rate brachytherapy planning in the treatment of cervical cancer has improved locoregional control and survival rates while reducing late morbidity [65]. External beam radiation therapy (EBRT) is commonly used adjuvantly for endometrial cancer and as a component of definitive chemoradiation therapy followed by brachytherapy for cervical cancer. EBRT has traditionally been delivered in a large 4-field box technique due to the potential for large day-to-day motion of the uterus. More conformal techniques use large margins to encompass the range of motion of the uterus. MRIgRT for such gynecologic malignancies has the potential to reduce toxicity to OARs with daily adaptive planning [66]. PTV margins in these locations can be reduced from 1.5 to 0.5 cm with MRIgRT [67]. Case reports on the treatment of cervical cancer with MRIgRT without daily adaptation show considerable movement in the PTV and shrinkage of the gross tumor volume over the course of radiation [68,69].

A challenge in treating gynecologic malignancies with MRIgRT is the limited field size for treatment. The integration of the linear accelerator with the MRI results in a smaller maximum treatable field size compared to that of a conventional linear accelerator. On the 1.5-T and 0.35-T MR-linac, the maximum superior-inferior direction field size is 22 cm and 24 cm, respectively. Sites with extensive targets in the cranial-caudal direction, including gynecologic malignancies and HN malignancies, do not fit in the MRIgRT treatment field in

40% of cases [2,70]. In addition, magnetic field inhomogeneities cause geometric distortions outside the treatment isocenter. On the 0.35-T MR-linac, although there are less than 1-mm distortions within a 10-cm radius of the isocenter, at 20 to 25 cm from the isocenter the distortions can be up to 7 mm [71]. A potential option for overcoming the limited field size with MRIgRT is to use 2 isocenters [70].

## OTHER SITES (LIVER, RECTUM, AND SARCOMA) AND MRI ARTIFACTS

Tumors within the liver, including hepatocellular carcinoma, cholangiocarcinoma, and metastases, are difficult to visualize on CBCT because of respiratory motion and poor soft tissue contrast. Consequently, larger margins are often required to account for the uncertainty in the tumor position. Although MRIgRT is better at visualizing the tumor, soft tissue contrast can further be enhanced with the use of gadohexetate intravenous contrast [72]. In a retrospective review of 26 patients with metastatic liver lesions and hepatocellular carcinomas treated with cobalt-based MRIgRT SABR to a median dose of 50 Gy in 5 fractions, the 2-year overall survival was 60% and 21-month local control was 80%, without any grade ≥4 toxicities [73]. In a study of 17 patients with unresectable locally advanced cholangiocarcinoma treated with cobalt-based MRIgRT SABR with a median dose of 40 Gy in 5 fractions, the 2-year overall survival was 46%, and local control was 73%, without any grade ≥4 toxicities [74]. Colorectal metastases to the liver have lower control rates compared with other types of histology [75]. The potential for safe dose escalation to colorectal metastases using an isotoxic approach on the MR-linac is currently being investigated (NCT04020276).

In locally advanced rectal cancer, the combination of preoperative chemotherapy and chemoradiation can increase the rate of complete pathologic response, and trials are being conducted to investigate nonoperative “watch and wait” strategies [76]. Rectal cancers have considerable variability in bowel and bladder filling. MRIgRT can enable safe dose-escalation strategies and help determine the best candidates for nonoperative management through the use of quantitative biomarkers [77,78].

MRIs of extremity soft tissue sarcomas are recommended to delineate the gross tumor volume (GTV) and peritumoral edema for preoperative radiotherapy [79]. The Phase III EORTC STRASS trial failed to show a benefit in preoperative radiotherapy for retroperitoneal sarcomas [80]. Alternative approaches to improving local control for retroperitoneal sarcomas include the use of MR-guided hypofractionated radiation 60 Gy in 3 to 8 fractions (NCT03972930). MR-guided radiation has also been used to treat challenging cases, including a pediatric rhabdomyosarcoma of the diaphragm and a left ventricle cardiac fibroma [81–83].

Although MRI has excellent soft tissue contrast and does not involve ionizing radiation, it can suffer from a range of imaging artifacts. Periodic respiratory motion can create a “ghosting” artifact, a faint repetition of structures across the image. Strategies such as breath-holds or detecting the position of the diaphragm can reduce these motion artifacts. Another broad category of artifacts is geometric distortion due to magnetic field inhomogeneity. Structures in the image can be represented in the wrong location. Certain

image sequences, such as diffusion weighted imaging (DWI), are particularly susceptible to geometric distortion, and caution should be exercised when targeting lesions based on DWI. Metal objects are generally restricted from MRIs, as they can be pro-pelled by large magnetic forces. MR-compatible metallic prostheses and devices can cause dark “banding” artifacts that distort the image near the object, which can be especially relevant for patients with sarcoma [84]. Even iron supplements and iron-fortified cereals can cause banding artifacts, and patients should be instructed to avoid consuming these during abdominal radiation (Fig. 5) [85].

## DISCUSSION

This review summarizes the clinical applications of MRIgRT, progress made so far, and areas under investigation. We have highlighted physics problems and technical challenges and opportunities that should be further explored for MRIgRT to reach its full potential. Although there are many dosimetric studies, most of the clinical experiences reported have been with 0.35-T cobalt-based MRIgRT, and outcomes focus mainly on acute toxicity rates, which have been favorable.

The MR-linac units are approximately twice the cost of a well-equipped conventional linear accelerator. To justify the purchase of these more expensive units, cancer centers must coordinate efforts to demonstrate favorable clinical outcomes [86]. MRIgRT can improve the therapeutic ratio, and the operational costs will likely shrink with the use of automation to expedite the adaptive workflow and with shorter hypofractionated treatments [87]. Multi-institutional trials and coordinated efforts will be essential to establishing MR-guided radiotherapy as a treatment option for patients with cancer globally.

## Supplementary Material

Refer to Web version on PubMed Central for supplementary material.

## DISCLOSURE

Dr S.L. Lee reports receiving travel reimbursement support from ViewRay. W.A. Hall receives departmental research and travel support from Elekta AB, and has a K grant from the National Institutes of Health (NIH). The project described was supported by the National Center for Advancing Translational Sciences, NIH, Award Number KL2TR001438. The content is solely the responsibility of the author(s) and does not necessarily represent the official views of NIH. Dr Z. S. Morris reports personal fees from ViewRay, outside the submitted work; Member of Scientific Advisory Board, Archeus Technologies; and on the Scientific Advisory Board for Seneca Therapeutics. Dr M. Bassetti reports meeting travel reimbursement support from ViewRay, and Clinical Trial Support from Merck, AstraZeneca, and EMD Serono.

## REFERENCES

[1]. Pollard JM, Wen Z, Sadagopan R, et al. The future of image-guided radiotherapy will be MR guided. Br J Radiol 2017;90:20160667. [PubMed: 28256898]

[2]. Klüter S Technical design and concept of a 0.35 T MR-Linac. Clin Transl Radiat Oncol 2019;18:98–101. [PubMed: 31341983]

[3]. Lagendijk JJW, Raaymakers BW, van Vulpen M. The magnetic resonance imaging–linac system. Semin Radiat Oncol 2014;24:207–9. [PubMed: 24931095]

[4]. Mutic S, Dempsey JF. The ViewRay system: magnetic resonance–guided and controlled radiotherapy. Semin Radiat Oncol 2014;24:196–9. [PubMed: 24931092]

[5]. Henke LE, Contreras JA, Green OL, et al. Magnetic resonance image-guided radiotherapy (MRIgRT): a 4.5-year clinical experience. Clin Oncol(R Coll Radiol) 2018; 30:720–7. [PubMed: 30197095]

[6]. Raaymakers BW, Jürgenliemk-Schulz IM, Bol GH, et al. First patients treated with a 1.5 T MRI-Linac: clinical proof of concept of a high-precision, high-field MRI guided radiotherapy treatment. Phys Med Biol 2017;62: L41–50. [PubMed: 29135471]

[7]. Koay EJ, Hanania AN, Hall WA, et al. Dose-Escalated Radiation Therapy for Pancreatic Cancer: A Simultaneous Integrated Boost Approach. Pr Radiat Oncol 2020;10: e495–507.

[8]. Reyngold M, Parikh P, Crane CH. Ablative radiation therapy for locally advanced pancreatic cancer: techniques and results. Radiat Oncol 2019;14:95. [PubMed: 31171025]

[9]. Boldrini L, Cusumano D, Cellini F, et al. Online adaptive magnetic resonance guided radiotherapy for pancreatic cancer: state of the art, pearls and pitfalls. Radiat Oncol 2019;14:71. [PubMed: 31036034]

[10]. Luterstein E, Cao M, Lamb J, et al. Stereotactic MRI-guided Adaptive Radiation Therapy (SMART) for locally advanced pancreatic cancer: a promising approach. Cureus 2018;10:e2324. [PubMed: 29765792]

[11]. Bohoudi O, Bruynzeel AME, Senan S, et al. Fast and robust online adaptive planning in stereotactic MR-guided adaptive radiation therapy (SMART) for pancreatic cancer. Radiother Oncol 2017;125:439–44. [PubMed: 28811038]

[12]. Bohoudi O, Bruynzeel AME, Meijerink MR, et al. Identification of patients with locally advanced pancreatic cancer benefitting from plan adaptation in MR-guided radiation therapy. Radiother Oncol 2019;132:16–22. [PubMed: 30825964]

[13]. Rudra S, Jiang N, Rosenberg SA, et al. Using adaptive magnetic resonance image-guided radiation therapy for treatment of inoperable pancreatic cancer. Cancer Med 2019;8:2123–32. [PubMed: 30932367]

[14]. Maurer T, Eiber M, Schwaiger M, et al. Current use of PSMA–PET in prostate cancer management. Nat Rev Urol 2016;13:226–35. [PubMed: 26902337]

[15]. De Michino S, Aparnathi M, Rostami A, et al. The utility of liquid biopsies in radiation oncology. Int J Radiat Oncol 2020;107(5):873–86.

[16]. Palma DA, Olson R, Harrow S, et al. Stereotactic ablative radiotherapy versus standard of care palliative treatment in patients with oligometastatic cancers (SABR-COMET): a randomised, phase 2, open-label trial. Lancet 2019; 393:2051–8. [PubMed: 30982687]

[17]. Winkel D, Bol GH, Werensteijn-Honingh AM, et al. Target coverage and dose criteria based evaluation of the first clinical 1.5T MR-linac SBRT treatments of lymph node oligometastases compared with conventional CBCT-linac treatment. Radiother Oncol 2020;146:118–25. [PubMed: 32146257]

[18]. Palacios MA, Bohoudi O, Bruynzeel AME, et al. Role of daily plan adaptation in MR-guided stereotactic ablative radiation therapy for adrenal metastases. Int J Radiat Oncol 2018;102:426–33.

[19]. Henke L, Kashani R, Robinson C, et al. Phase I trial of stereotactic MR-guided online adaptive radiation therapy (SMART) for the treatment of oligometastatic or unresectable primary malignancies of the abdomen. Radiother Oncol 2018;126:519–26. [PubMed: 29277446]

[20]. Hansen AT, Poulsen PR, Høyer M, et al. Isotoxic dose prescription level strategies for stereotactic liver radiotherapy: the price of dose uniformity. Acta Oncol 2020;59:558–64. [PubMed: 31833432]

[21]. Bainbridge HE, Menten MJ, Fast MF, et al. Treating locally advanced lung cancer with a 1.5T MR-Linac - Effects of the magnetic field and irradiation geometry on conventionally fractionated and isotoxic dose-escalated radiotherapy. Radiother Oncol 2017;125:280–5. [PubMed: 28987747]

[22]. Zhao Q, Liu M, Wang Z, et al. High dose radiation therapy based on normal tissue constraints with concurrent chemotherapy achieves promising survival of patients with unresectable stage III non-small cell lung cancer. Radiother Oncol 2020;145:7–12. [PubMed: 31869678]

[23]. De Ruysscher D, van Baardwijk A, Wanders R, et al. Individualized accelerated isotoxic concurrent chemoradiotherapy for stage III non-small cell lung cancer: 5-year results of a prospective study. Radiother Oncol 2019;135:141–6. [PubMed: 31015160]

[24]. Cao Y, Tseng C-L, Balter JM, et al. MR-guided radiation therapy: transformative technology and its role in the central nervous system. Neuro Oncol 2017;19:ii16–29. [PubMed: 28380637]

[25]. Zeng KL, Tseng C-L, Soliman H, et al. Stereotactic body radiotherapy (SBRT) for oligometastatic spine metastases: an overview. Front Oncol 2019;9:337. [PubMed: 31119099]

[26]. Mehta S, Gajjar SR, Padgett KR, et al. Daily tracking of glioblastoma resection cavity, cerebral edema, and tumor volume with MRI-guided radiation therapy. Cureus 2018;10:e2346. [PubMed: 29796358]

[27]. van der Heide UA, Thorwarth D. Quantitative imaging for radiation oncology. Int J Radiat Oncol 2018;102: 683–6.

[28]. Gao Y, Han F, Zhou Z, et al. Distortion-free diffusion MRI using an MRI-guided Tri-Cobalt 60 radiotherapy system: sequence verification and preliminary clinical experience. Med Phys 2017;44:5357–66. [PubMed: 28692129]

[29]. Kim MM, Parmar HA, Aryal MP, et al. Developing a pipeline for multiparametric MRI-guided radiation therapy: initial results from a Phase II clinical trial in newly diagnosed glioblastoma. Tomography 2019;5:118–26. [PubMed: 30854449]

[30]. Kaanders JHAM, van den Bosch S, Dijkema T, et al. Advances in cancer imaging require renewed radiotherapy dose and target volume concepts. Radiother Oncol 2020;148:140–2. [PubMed: 32361663]

[31]. Hall WA, Paulson ES, van der Heide UA, et al. The transformation of radiation oncology using real-time magnetic resonance guidance: a review. Eur J Cancer 2019; 122:42–52. [PubMed: 31614288]

[32]. Bhujwalla ZM, Kakkad S, Chen Z, et al. Theranostics and metabolotheranostics for precision medicine in oncology. J Magn Reson 2018;291:141–51. [PubMed: 29705040]

[33]. Raghavan G, Kishan AU, Cao M, et al. Anatomic and dosimetric changes in patients with head and neck cancer treated with an integrated MRI-tri-60Co teletherapy device. Br J Radiol 2016;89:20160624. [PubMed: 27653787]

[34]. Chen AM, Hsu S, Lamb J, et al. MRI-guided radiotherapy for head and neck cancer: initial clinical experience. Clin Transl Oncol 2018;20:160–8. [PubMed: 28612199]

[35]. Bahig H, Yuan Y, Mohamed ASR, et al. Magnetic Resonance-based Response Assessment and Dose Adaptation in Human Papilloma Virus Positive Tumors of the Oropharynx treated with Radiotherapy (MR-ADAPTOR): an R-IDEAL stage 2a-2b/Bayesian phase II trial. Clin Transl Radiat Oncol 2018;13:19–23. [PubMed: 30386824]

[36]. Thompson RF, Valdes G, Fuller CD, et al. Artificial intelligence in radiation oncology: a specialty-wide disruptive transformation? Radiother Oncol 2018;129:421–6. [PubMed: 29907338]

[37]. Meyer P, Noblet V, Mazzara C, et al. Survey on deep learning for radiotherapy. Comput Biol Med 2018;98: 126–46. [PubMed: 29787940]

[38]. Walker GV, Awan M, Tao R, et al. Prospective randomized double-blind study of atlas-based organ-at-risk autosegmentation-assisted radiation planning in head and neck cancer. Radiother Oncol 2014;112:321–5. [PubMed: 25216572]

[39]. Cardenas CE, McCarroll RE, Court LE, et al. Deep learning algorithm for auto-delineation of high-risk oropharyngeal clinical target volumes with built-in dice similarity coefficient parameter optimization function. Int J Radiat Oncol 2018;101(2):468–78.

[40]. Tong N, Gou S, Yang S, et al. Shape constrained fully convolutional DenseNet with adversarial training for multiorgan segmentation on head and neck CT and low-field MR images. Med Phys 2019;46:2669–82. [PubMed: 31002188]

[41]. Whelan TJ, Pignol J-P, Levine MN, et al. Long-term results of hypofractionated radiation therapy for breast cancer. N Engl J Med 2010;362:513–20. [PubMed: 20147717]

[42]. Poppe MM, Yehia ZA, Baker C, et al. 5-year update of a multi institution prospective Phase II hypofractionated post-mastectomy radiation therapy trial. Int J Radiat Oncol 2020;107(4):694–700.

[43]. Brunt AM, Haviland JS, Wheatley DA, et al. Hypofractionated breast radiotherapy for 1 week versus 3 weeks (FAST-Forward): 5-year efficacy and late normal tissue effects results from a multicentre, non-inferiority, randomised, phase 3 trial. Lancet 2020;395(10237):1613–26. [PubMed: 32580883]

[44]. Vicini FA, Cecchini RS, White JR, et al. Long-term primary results of accelerated partial breast irradiation after breast-conserving surgery for early-stage breast cancer: a randomised, phase 3, equivalence trial. Lancet 2019;394:2155–64. [PubMed: 31813636]

[45]. Whelan TJ, Julian JA, Berrang TS, et al. External beam accelerated partial breast irradiation versus whole breast irradiation after breast conserving surgery in women with ductal carcinoma in situ and node-negative breast cancer (RAPID): a randomised controlled trial. Lancet 2019;394:2165–72. [PubMed: 31813635]

[46]. van Heijst TC, Philippens ME, Charaghvandi RK, et al. Quantification of intra-fraction motion in breast radiotherapy using supine magnetic resonance imaging. Phys Med Biol 2016;61:1352–70. [PubMed: 26797074]

[47]. Jeon SH, Shin KH, Park SY, et al. Seroma change during magnetic resonance imaging-guided partial breast irradiation and its clinical implications. Radiat Oncol 2017; 12:103. [PubMed: 28633637]

[48]. Vasmel JE, Charaghvandi RK, Houweling AC, et al. Tumor response after neoadjuvant magnetic resonance guided single ablative dose partial breast irradiation. Int J Radiat Oncol 2020;106:821–9.

[49]. den Hartogh MD, Philippens ME, van Dam IE, et al. MRI and CT imaging for preoperative target volume delineation in breast-conserving therapy. Radiat Oncol 2014;9: 63. [PubMed: 24571783]

[50]. Acharya S, Fischer-Valuck BW, Mazur TR, et al. Magnetic resonance image guided radiation therapy for external beam accelerated partial-breast irradiation: evaluation of delivered dose and intrafractional cavity motion. Int J Radiat Oncol 2016;96:785–92.

[51]. Park JM, Shin KH, Kim JI, et al. Air-electron stream interactions during magnetic resonance IGRT: Skin irradiation outside the treatment field during accelerated partial breast irradiation. Strahlenther Onkol 2018;194:50–9. [PubMed: 28916952]

[52]. Kennedy WR, Thomas MA, Stanley JA, et al. Single Institution Phase I/II prospective clinical trial of single fraction high gradient adjuvant partial breast irradiation for hormone sensitive stage 0-i breast cancer. Int J Radiat Oncol • Biol • Phys 2020;107(2):344–52. [PubMed: 32084524]

[53]. Charaghvandi RK, van Asselen B, Philippens ME, et al. Redefining radiotherapy for early-stage breast cancer with single dose ablative treatment: a study protocol. BMC Cancer 2017;17:181. [PubMed: 28274211]

[54]. Nachbar M, Mönnich D, Boeke S, et al. Partial breast irradiation with the 1.5 T MR-Linac: first patient treatment and analysis of electron return and stream effects. Radiother Oncol 2020;145:30–5. [PubMed: 31874347]

[55]. Kubota T, Araki F, Ohno T. Impact of inline magnetic fields on dose distributions for VMAT in lung tumor. Phys Med 2019;59:100–6. [PubMed: 30928057]

[56]. Kim A, Lim-Reinders S, McCann C, et al. Magnetic field dose effects on different radiation beam geometries for hypofractionated partial breast irradiation. J Appl Clin Med Phys 2017;18:62–70.

[57]. Timmerman R, Paulus R, Galvin J, et al. Stereotactic body radiation therapy for inoperable early stage lung cancer. JAMA 2010;303:1070–6. [PubMed: 20233825]

[58]. Henke LE, Olsen JR, Contreras JA, et al. Stereotactic MR-Guided Online Adaptive Radiation Therapy (SMART) for ultracentral thorax malignancies: results of a Phase 1 trial. Adv Radiat Oncol 2019;4:201–9. [PubMed: 30706029]

[59]. Finazzi T, Haasbeek CJA, Spoelstra FOB, et al. Clinical outcomes of stereotactic MR-guided adaptive radiation therapy for high-risk lung tumors. Int J Radiat Oncol Biol Phys 2020;107(2):270–8. [PubMed: 32105742]

[60]. Park JM, Wu HG, Kim HJ, et al. Comparison of treatment plans between IMRT with MR-linac and VMAT for lung SABR. Radiat Oncol 2019;14:105. [PubMed: 31196120]

[61]. Daşu A. Is the α/β value for prostate tumours low enough to be safely used in clinical trials? Clin Oncol 2007;19:289–301.

[62]. Alongi F, Rigo M, Figlia V, et al. 1.5 T MR-guided and daily adapted SBRT for prostate cancer: feasibility, preliminary clinical tolerability, quality of life and patient-reported outcomes during treatment. Radiat Oncol 2020;15:69. [PubMed: 32248826]

[63]. Bruynzeel AME, Tetar SU, Oei SS, et al. A prospective single-arm phase 2 study of stereotactic magnetic resonance guided adaptive radiation therapy for prostate cancer: early toxicity results. Int J Radiat Oncol 2019;105: 1086–94.

[64]. Edmund JM, Nyholm T. A review of substitute CT generation for MRI-only radiation therapy. Radiat Oncol 2017;12:28. [PubMed: 28126030]

[65]. Rijkmans EC, Nout RA, Rutten IHHM, et al. Improved survival of patients with cervical cancer treated with image-guided brachytherapy compared with conventional brachytherapy. Gynecol Oncol 2014;135:231–8. [PubMed: 25172763]

[66]. Cree A, O'Donovan A, O'Hanlon S. New horizons in radiotherapy for older people. Age Ageing 2019;48: 605–12. [PubMed: 31361801]

[67]. Visser J, de Boer P, Crama KF, et al. Dosimetric comparison of library of plans and online MRI-guided radiotherapy of cervical cancer in the presence of intrafraction anatomical changes. Radiat Oncol 2019; 14:126. [PubMed: 31300000]

[68]. Asher D, Padgett KR, Llorente RE, et al. Magnetic resonance-guided external beam radiation and brachytherapy for a patient with intact cervical cancer. Cureus 2018;10:e2577. [PubMed: 29984119]

[69]. Boldrini L, Chiloiro G, Pesce A, et al. Hybrid MRI guided radiotherapy in locally advanced cervical cancer: case report of an innovative personalized therapeutic approach. Clin Transl Radiat Oncol 2020;20:27–9. [PubMed: 31768423]

[70]. Chuter RW, Whitehurst P, Choudhury A, et al. Technical note: investigating the impact of field size on patient selection for the 1.5T MR-Linac. Med Phys 2017;44: 5667–71. [PubMed: 28869651]

[71]. Nejad-Davarani SP, Kim JP, Du D, et al. Large field of view distortion assessment in a low-field MR-linac. Med Phys 2019;46:2347–55. [PubMed: 30838680]

[72]. Wojcieszynski AP, Rosenberg SA, Brower JV, et al. Gadoxetate for direct tumor therapy and tracking with real-time MRI-guided stereotactic body radiation therapy of the liver. Radiother Oncol 2016;118:416–8. [PubMed: 26627702]

[73]. Rosenberg SA, Henke LE, Shaverdian N, et al. A multi-institutional experience of MR-guided liver stereotactic body radiation therapy. Adv Radiat Oncol 2019;4:142–9. [PubMed: 30706022]

[74]. Luterstein E, Cao M, Lamb JM, et al. Clinical outcomes using magnetic resonance–guided stereotactic body radiation therapy in patients with locally advanced cholangiocarcinoma. Adv Radiat Oncol 2019;5(2):189–95. [PubMed: 32280818]

[75]. Ahmed KA, Caudell JJ, El-Haddad G, et al. Radiosensitivity differences between liver metastases based on primary histology suggest implications for clinical outcomes after stereotactic body radiation therapy. Int J Radiat Oncol 2016;95:1399–404.

[76]. Cercek A, Roxburgh CSD, Strombom P, et al. Adoption of total neoadjuvant therapy for locally advanced rectal cancer. JAMA Oncol 2018;4:e180071. [PubMed: 29566109]

[77]. Gani C, Boldrini L, Valentini V. Online MR guided radiotherapy for rectal cancer. New opportunities. Clin Transl Radiat Oncol 2019;18:66–7. [PubMed: 31341978]

[78]. Chand M, Oliva Perez R. MRI linac and how it may potentially lead to more complete response in rectal cancer. Dis Colon Rectum 2018;61:643–4. [PubMed: 29722720]

[79]. Haas RLM, DeLaney TF, O'Sullivan B, et al. Radiotherapy for management of extremity soft tissue sarcomas: why, when, and where? Int J Radiat Oncol Biol Phys 2012; 84:572–80. [PubMed: 22520481]

[80]. Bonvalot S, Gronchi A, Le Pechoux C, et al. STRASS (EORTC 62092): A phase III randomized study of preoperative radiotherapy plus surgery versus surgery alone for patients with retroperitoneal sarcoma. J Clin Oncol 2019;37:11001.

[81]. Kishan AU, Cao M, Mikaeilian AG, et al. Dosimetric feasibility of magnetic resonance imaging-guided tri-cobalt 60 preoperative intensity modulated radiation therapy for soft tissue sarcomas of the extremity. Pr Radiat Oncol 2015;5:350–6.

[82]. Henke LE, Green OL, Schiff J, et al. First reported case of pediatric radiation treatment with magnetic resonance image guided radiation therapy. Adv Radiat Oncol 2019;4:233–6. [PubMed: 31011667]

[83]. Gach HM, Green OL, Cuculich PS, et al. Lessons learned from the first human low-field MRI guided radiation therapy of the heart in the presence of an implantable cardiac defibrillator. Pr Radiat Oncol 2019;9:274–9.

[84]. van der Heide UA, Frantzen-Steneker M, Astreinidou E, et al. MRI basics for radiation oncologists. Clin Transl Radiat Oncol 2019;18:74–9. [PubMed: 31341980]

[85]. Green O, Henke LE, Parikh P, et al. Practical implications of ferromagnetic artifacts in low-field MRI-guided radiotherapy. Cureus 2018;10:e2359. [PubMed: 29805928]

[86]. Noble DJ, Burnet NG. The future of image-guided radiotherapy-is image everything? Br J Radiol 2018;91: 20170894. [PubMed: 29616822]

[87]. Bayouth JE, Low DA, Zaidi H. MRI-linac systems will replace conventional IGRT systems within 15 years. Med Phys 2019;46:3753–6. [PubMed: 31199516]

**KEY POINTS**

- Integrated MRI-guided radiation therapy (MRIgRT) systems have recently been developed with growing clinical adoption since 2014.
- MRIgRT systems have superior soft tissue contrast and are capable of real-time treatment gating and on-table radiation plan adaptation.
- MRIgRT presents many technical challenges but has great potential to improve the therapeutic ratio of radiation treatment.
- MRIgRT can be used to treat malignancies in all body sites, although long-term clinical outcomes are currently pending.
- Collective efforts will be required to demonstrate improved clinical outcomes to offset the increased cost of MRIgRT systems.

## CLINICS CARE POINTS

- MRIgRT systems have superior soft tissue contrast and are capable of more accurate and precise treatments with real-time imaging and treatment gating during radiation delivery and with radiation plan adaptation while the patient is on the treatment table.
- MRIgRT presents many technical challenges but has great potential to improve the therapeutic ratio of radiation treatment.
- Collective efforts will be required to demonstrate improved clinical outcomes to offset the increased cost of MRIgRT systems.

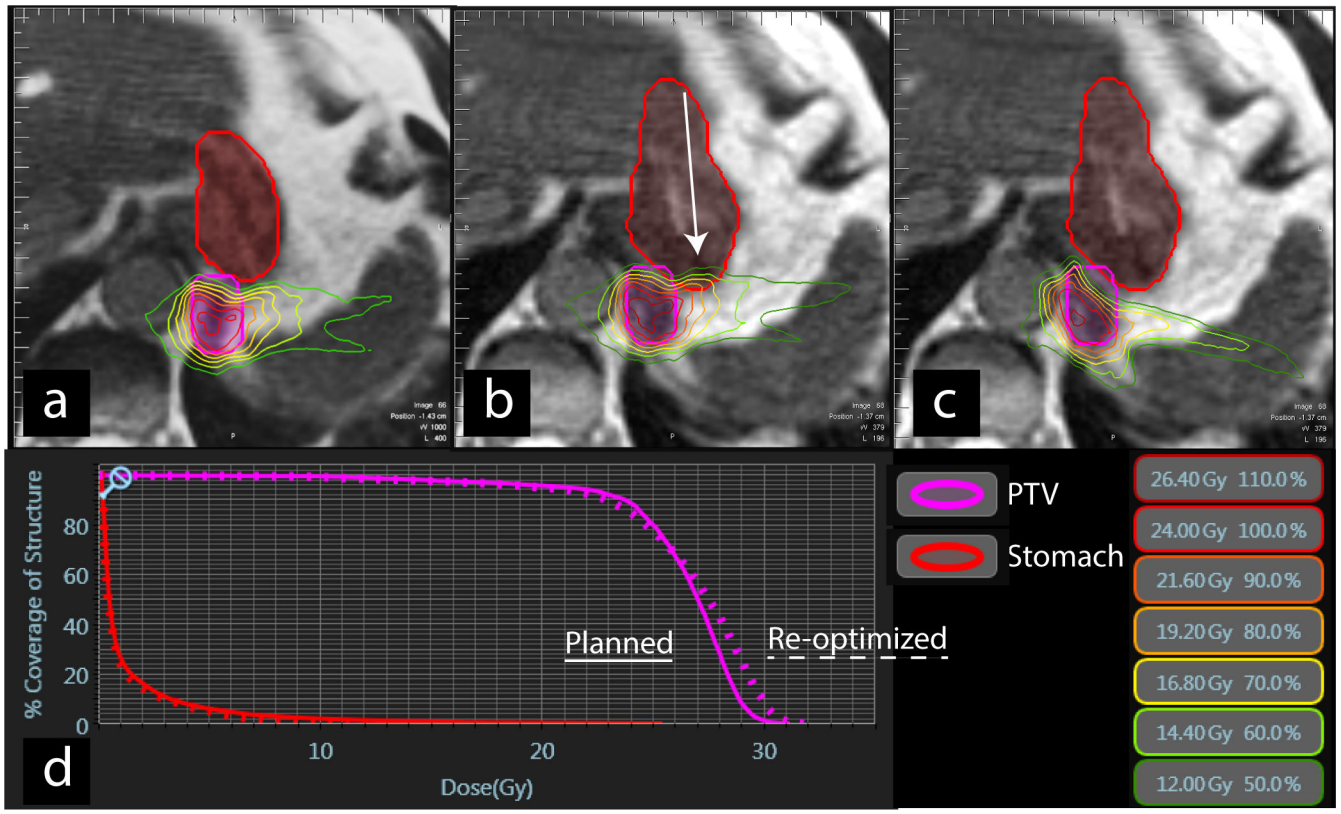


**FIG. 1.**

Axial views of SABR dose distribution for an oligometastatic lesion in left lower lung close to the stomach at (**A**) initial MRI simulation, (**B**) day of treatment before plan adaptation, and (**C**) after plan adaptation to avoid overdosing the stomach (*arrow*) (D) DVH demonstrating an increase in dose to the planning target volume (PTV) after re-optimization. See Video 1 for sagittal cine of tumor tracking. Pink = Planning target volume, red = stomach. DVH, Dose volume histogram; SABR, stereotactic ablative radiotherapy.

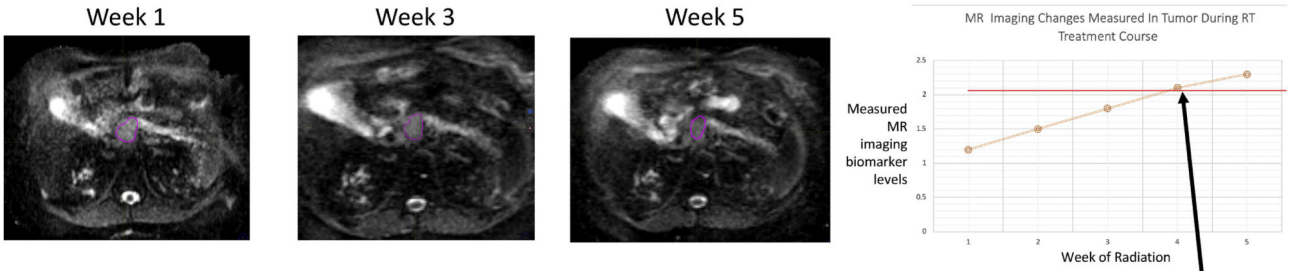


**FIG. 2.**

Hypothesized imaging biomarker “threshold” goal (*arrow*) for a radiation treatment dosing. Imaging response during treatment could be closely correlated with a validated imaging biomarker and clinical/pathologic end-point. (*Adapted from* Hall WA, Paulson ES, van der Heide UA, et al. The transformation of radiation oncology using real-time magnetic resonance guidance: A review. Eur. J. Cancer. 2019;122:42–52.; with permission. (Figure 3 in original).)

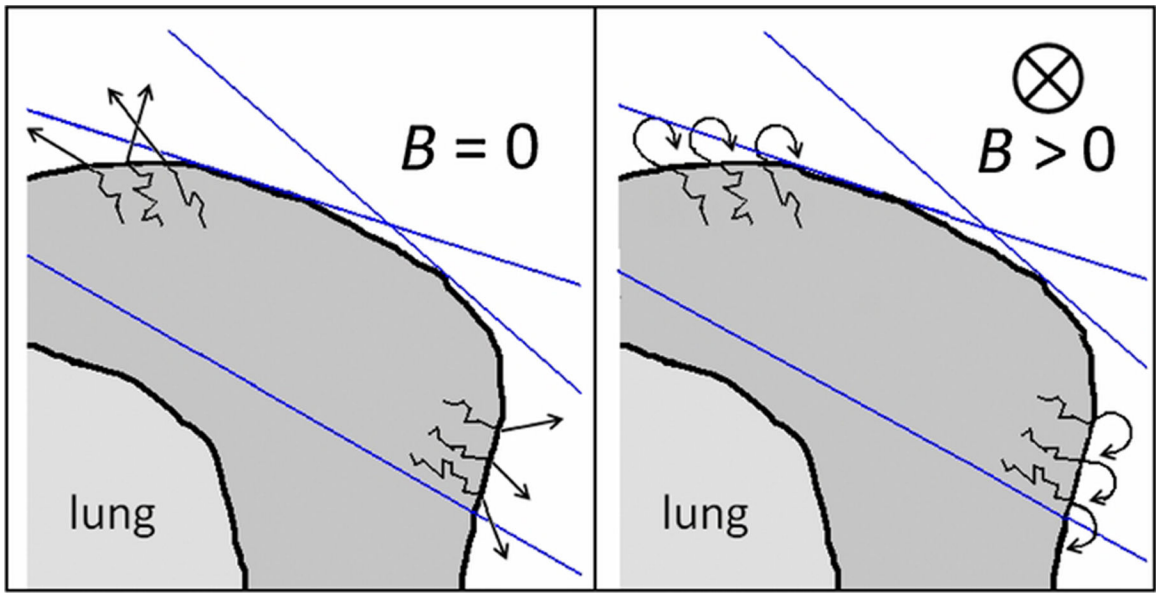


**FIG. 3.**

Illustration of the electron return effect, for left whole breast irradiation by means of 2 tangential fields. The edges of the photon beams are depicted by the blue lines. (*Left*) In the absence of a magnetic field, secondary electrons leave the breast at the tissue-air interface. (*Right*) With a magnetic field, secondary electrons return to the breast, increasing the skin dose. (*From* van Heijst T, den Hartogh M, J W Lagendijk J, et al. MR-guided breast radiotherapy: Feasibility and magnetic-field impact on skin dose. Phys. Med. Biol. 2013;58:5917–5930 © Institute of Physics and Engineering in Medicine. Reproduced by permission of IOP Publishing. All rights reserved.)

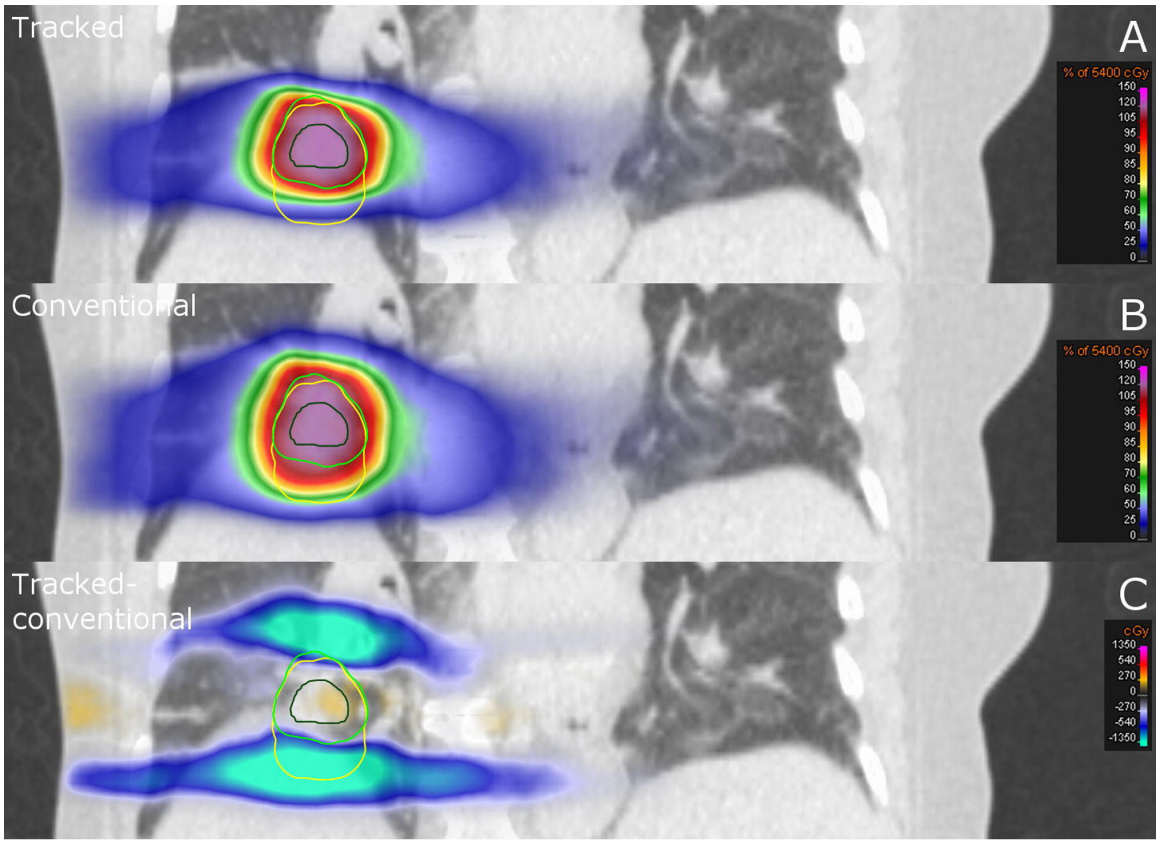


**FIG. 4.**

Coronal CT slice of a patient with lung cancer. Dose distribution of (**A**) respiratory gated treatment in which the tumor is tracked and (**B**) conventional free-breathing treatment with larger treatment margins. (**C**) Dose difference between the tracked treatment versus the conventional treatment. (*From* Menten MJ, Fast MF, Nill S, et al. Lung stereotactic body radiotherapy with an MR-linac – Quantifying the impact of the magnetic field and real-time tumor tracking. Radiother. Oncol. 2016;119:461–466.; with permission. (Figure 4 in original).)

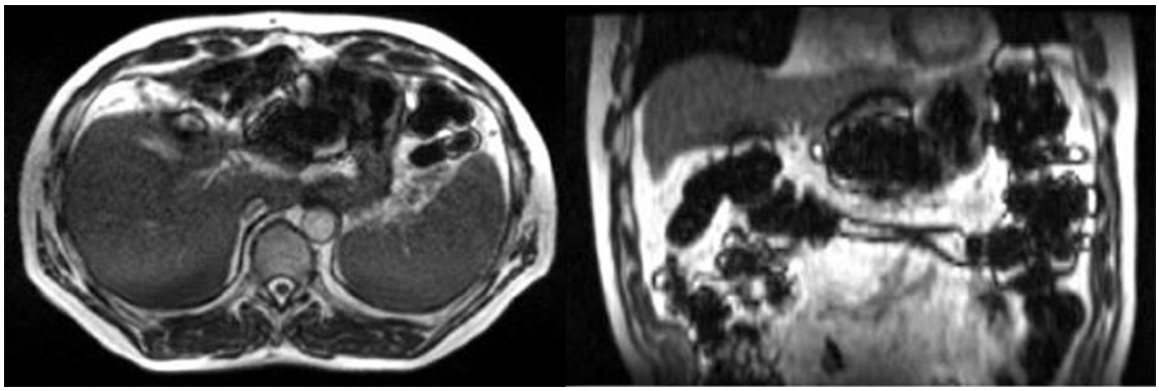

**FIG. 5.**

(*Left*) Axial and (*right*) coronal views of a patient a few hours after ingesting iron-fortified breakfast cereal causing susceptibility artifact. (*From* Green O, Henke LE, Parikh P, et al. Practical Implications of Ferromagnetic Artifacts in Low-field MRI-guided Radiotherapy. Cureus. 2018;10:e2359.; with permission. (Figure 2 in original).)